CHALMERS

Citation for the published paper:

Author(s): Healy SB, O'Reilly EP, Gustavsson JS, Westbergh P, Haglund A, Larsson A, Joel A
Source: IEEE JOURNAL OF QUANTUM ELECTRONICS
Volume: 46 Issue: 4 Pages: 506-512
Published: APR 2010

Active Region Design for High-Speed 850-nm VCSELs

Sorcha B. Healy, Eoin P. O'Reilly, Johan S. Gustavsson, Petter Westbergh, Åsa Haglund, Anders Larsson, and Andrew Joel

***Abstract*—Higher speed short-wavelength (850 nm) VCSELs are required for future high-capacity, short-reach data communication links. The modulation bandwidth of such devices is intrinsically limited by the differential gain of the quantum wells (QWs) used in the active region. We present gain calculations using an 8-band k·p Hamiltonian which show that the incorporation of 10% In in an InGaAs/AlGaAs QW structure can approximately double the differential gain compared to a GaAs/AlGaAs QW structure, with little additional improvement achieved by further increasing the In composition in the QW. This improvement is confirmed by extracting the differential gain value from measurements of the modulation response of VCSELs with optimized InGaAs/AlGaAs QW and conventional GaAs/AlGaAs QW active regions. Excellent agreement is obtained between the theoretically and experimentally determined values of the differential gain, confirming the benefits of strained InGaAs QW structures for high-speed 850-nm VCSEL applications.**

***Index Terms*—Differential gain, high speed, vertical-cavity surface-emitting laser (VCSEL).**

I. Introduction

To meet the demands for higher communication capacity and low power consumption in short reach optical links and interconnects, GaAs-based vertical cavity surface emitting lasers (VCSELs) are being developed for operation at enhanced speed [1], [2]. Direct current modulation of VCSELs at bit rates as high as 40 Gb/s was recently demonstrated at wavelengths of 850 and 1100 nm [3], [4]. The former (850 nm) is of particular importance since it has become the standard wavelength for data communication links. Therefore, high-speed multimode fiber is available, and standards are being developed for this wavelength.

Manuscript received October 06, 2009; revised November 19, 2009. Current version published February 17, 2010. This work was supported by the European project VISIT (FP7-224211), by the Swedish Foundation for Strategic Research (SSF) and by Science Foundation Ireland (SFI).

S. B. Healy is with the Tyndall National Institute, Lee Maltings, Cork, Ireland (e-mail: sorcha.healy@tyndall.ie).

E. P. O'Reilly is with the Tyndall National Institute, Lee Maltings, Cork, Ireland, and also with the Department of Physics, University College Cork, Ireland (e-mail: eoin.oreilly@tyndall.ie).

J. S. Gustavsson, P. Westbergh, Å. Haglund, and A. Larsson are with the Photonics Laboratory, Department of Microtechnology and Nanoscience, Chalmers University of Technology, SE-412 96 Göteborg, Sweden (e-mail: johan.gustavsson@chalmers.se; petter.westbergh@chalmers.se; asa.haglund@chalmers.se; anders.larsson@chalmers.se).

A. Joel is with IQE Europe Ltd., Cardiff, CF3 0LW, U.K. (e-mail: AJoel@IQEP.com).

Color versions of one or more of the figures in this paper are available online at http://ieeexplore.ieee.org.

Digital Object Identifier 10.1109/JQE.2009.2038176

The modulation bandwidth of a VCSEL (as of any other semiconductor laser) is fundamentally limited by the rates at which the resonance frequency and the damping of the resonant carrier–photon interaction increase with current. Initially, the modulation bandwidth increases because of the increasing resonance frequency, but eventually the damping becomes large enough to limit the bandwidth. This defines the intrinsic modulation bandwidth. With increasing current, the temperature of the active region starts to increase due to self-heating. This eventually leads to a saturation of the photon density and therefore the resonance frequency and the modulation bandwidth, which defines the thermally limited bandwidth. The intrinsic and thermally limited bandwidths are thus to a large degree limited by the rate at which the resonance frequency increases with current. This is primarily determined by the differential gain, with a higher differential gain resulting in a more rapid increase of the resonance frequency, thus enabling a higher modulation bandwidth to be reached before being limited by damping and/or thermal effects.

Of great importance for the design of high-speed VCSELs is, therefore, to maximize the differential gain. It is well known that strained quantum wells (QWs) can provide a higher differential gain, due to effects of both quantum confinement and strain [5], [6]. Strained QWs were previously employed for improving the high-speed characteristics of 850-nm VCSELs intended for operation at 10 Gb/s [7]. More recent VCSELs operating at higher speed (30–40 Gb/s) all use strained QWs [1]–[4], [8]–[10].

It is the aim of this work to find an optimum active region design for 850-nm datacom VCSELs employing strained InGaAs/AlGaAs QWs. The effects of QW thickness and strain (In concentration) on differential gain are analyzed using 8-band k · p theory. Under the condition of having the gain peak near 850 nm, designs that provide the most significant enhancement of the differential gain with respect to unstrained GaAs/AlGaAs QWs are identified. The improvement of differential gain is also confirmed by small-signal modulation response measurements on 850-nm VCSELs with strained InGaAs/AlGaAs and unstrained GaAs/AlGaAs QWs.

The paper is organized as follows. Section II describes the various designs considered in the theoretical and experimental studies. Results from band structure and gain calculations are presented in Section III and a comparison between theoretical and experimental values for differential gain are presented in Section IV. Conclusions are given in Section V.

II. Design

The active region of a conventional 850-nm VCSEL employs unstrained, multiple GaAs/AlGaAs QWs, with a QW thickness

TABLE I
ACTIVE REGION DESIGNS CONSIDERED IN THE CALCULATIONS OF ENERGY STATES, BAND DISPERSIONS, DENSITY OF STATES, AND GAIN CHARACTERISTICS. ALSO LISTED ARE THE OPTICAL CONFINEMENT FACTORS (Γ) IN THE VCSEL CAVITY

QW material	QW width (nm)	No. of QWs	Barrier material	Barrier width (nm)	Γ
GaAs	8.0	3	Al(0.30)GaAs	8	0.0346
In(0.10)GaAs	4.0	5	Al(0.37)GaAs	6	0.0289
In(0.12)GaAs	3.6	5	Al(0.37)GaAs	6	0.0260
In(0.15)GaAs	3.3	6	Al(0.37)GaAs	6	0.0286

of ∼8 nm and an Al concentration in the barriers of ∼30% [1]. When adding In to the QWs for improving differential gain, the QW thickness has to be reduced, and the Al concentration in the barriers has to be increased to maintain the gain peak at 850 nm. When using multiple InGaAs/AlGaAs QWs, the accumulated strain also has to be considered since the critical thickness must not be exceeded. In addition, with a too-high concentration of Al in the barriers, a significant population of X-related states in the conduction band occurs, which may slow down the trapping of electrons in the QW ground state, thus affecting the high-speed performance. In the present designs, we therefore limit the Al concentration in the barriers to 37% at which the occupation of X-related states was found to be negligible.

The QW designs considered are listed in Table I. The In concentration varies from 0 to 15%. To maintain the gain peak close to 850 nm, the Al concentration in the InGaAs/AlGaAs QWs is increased to 37%, and the QW thickness is reduced from 8 to 3.3 nm with increasing In concentration.

The VCSEL cavity is as described in [1]. The top p-doped distributed Bragg reflector (DBR) consists of 23 pairs of $Al_{0.90}Ga_{0.10}As/Al_{0.12}Ga_{0.88}As$ layers and the bottom n-doped DBR consists of four pairs of $Al_{0.90}Ga_{0.10}As/Al_{0.12}Ga_{0.88}As$ layers (closest to the active region) followed by an additional 28 pairs of $AlAs/Al_{0.12}Ga_{0.88}As$ layers (where the use of binary AlAs layers is expected to reduce the thermal impedance because of the higher thermal conductivity of binary materials compared to ternary). The longitudinal optical confinement factor was calculated using a one-dimensional transfer matrix method and was found to be 3.46% for the VCSEL with three GaAs/AlGaAs QWs. To maintain a similar optical confinement factor $(\sim 3\%)$ for the VCSELs with InGaAs/AlGaAs QWs, the number of QWs was increased from 3 to 6 with increasing In concentration and decreasing QW thickness. The number of QWs and the corresponding optical confinement factors are also listed in Table I. It is expected that none of the designs exceed the critical thickness limit.

III. THEORY

We use an 8-band k·p Hamiltonian [11] to determine the electronic structure of the InGaAs QW structures. The band structure is calculated using a plane-wave expansion method, where we surround each active region of N_w QWs (Table I) and $(N_w - 1)$ barriers with 20-nm AlGaAs external barriers, giving a supercell of length greater than 80 nm in all cases. We include 61 plane waves for each basis state to ensure convergence of the calculated band dispersion. We calculate the band dispersion using the axial approximation [12], so that the band dispersion is isotropic in the QW plane. The material parameters used in this work were taken from [13], with the exception of the band offsets, which were determined using Model Solid theory [14]. We calculate the material gain following a similar approach to that used in [11] and [15], using a sech broadening function when determining the gain, with the line broadening $\delta = 6.6$ meV and with the momentum matrix elements calculated fully following the method described in [16].

Fig. 1 shows the calculated valence band dispersion for the series of InGaAs/AlGaAs QW structures defined in Table I. The structures considered are (left to right) an 8-nm unstrained GaAs QW; a 4-nm $In_{0.10}Ga_{0.90}As$ QW; a 3.6-nm $In_{0.12}Ga_{0.88}As$ QW and a 3.3-nm $In_{0.15}Ga_{0.85}As$ QW. Table II lists the calculated ground state transition energy and wavelength for each of these structures at 25 °C and at 85 °C, confirming that all have an optical gap close to 850 nm. To facilitate comparison between the different graphs, the highest confined heavy-hole state, HH1, is in each case taken as the zero of energy. It can be seen that the unstrained GaAs material has a small splitting between the highest heavy-hole (HH) and light-hole (LH) state (21 meV; see Table II), with the splitting determined by the QW width and the difference in the growth direction hole effective masses. The addition of In to the QW increases the HH-LH splitting, both because of the strain-induced splitting of the HH and LH band edge states, and also because of the reduction in QW width required to maintain a fixed emission wavelength. The incorporation of 10% In in the QW (0.71% strain) increases the HH-LH splitting to 76 meV, while 12% In in the QW layer increases it further to 84 meV, with 15% In giving a calculated splitting of 95 meV.

Fig. 2 shows the calculated valence band density of states (DOS) for the four structures considered in Fig. 1. It can be seen that the addition of In significantly reduces the density of states near the valence band maximum, due to the increased separation and reduced band mixing between the highest HH and LH valence bands. This reduction in the valence band DOS near the band edge reduces the carrier density per unit area $n_{\mathrm{tr,2D}}$ required to reach transparency and will also lead to an improved differential gain in the In-containing QW structures [5]. It can be seen that the incorporation of 10% In leads to a reduced DOS over an energy range of about 75 meV (∼3 kT at room temperature T_{room}) with 15% In increasing this energy range to almost 100 meV (∼4 $\mathrm{kT_{room}}$). In addition, the combination of the increased In concentration in the QW and Al concentration in the barrier pushes the barrier valence band edge further away from the highest valence state in the QW, with this energy separation increasing from 130 meV in the GaAs/AlGaAs to over 200 meV in the InGaAs/AlGaAs QW structures. The major reduction in density of states has already

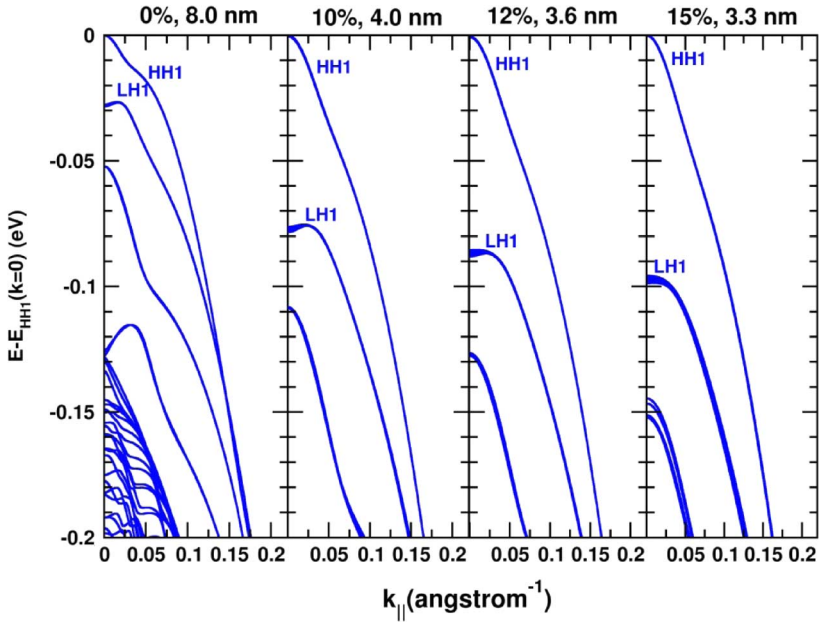

Fig. 1. Valence band dispersions for the QW structures defined in Table I.

TABLE II
ENERGIES AND CORRESPONDING WAVELENGTHS FOR THE GROUND STATE TRANSITIONS (E1-HH1) FOR THE QW DESIGNS IN TABLE I. ALSO LISTED IS THE SPLITTING OF HEAVY AND LIGHT HOLE GROUND STATES (HH1-LH1). NUMBERS IN PARENTHESES ARE AT 85 °C, OTHERS AT 25 °C

QW material	QW width (nm)	Barrier material	E1-HH1 (eV)	E1-HH1 (nm)	HH1-LH1 (meV)
GaAs	8.0	Al(0.30)GaAs	1.481 (1.455)	837 (852)	21
In(0.10)GaAs	4.0	Al(0.37)GaAs	1.474 (1.449)	841 (856)	76
In(0.12)GaAs	3.6	Al(0.37)GaAs	1.477 (1.452)	840 (854)	84
In(0.15)GaAs	3.3	Al(0.37)GaAs	1.469 (1.444)	844 (859)	95

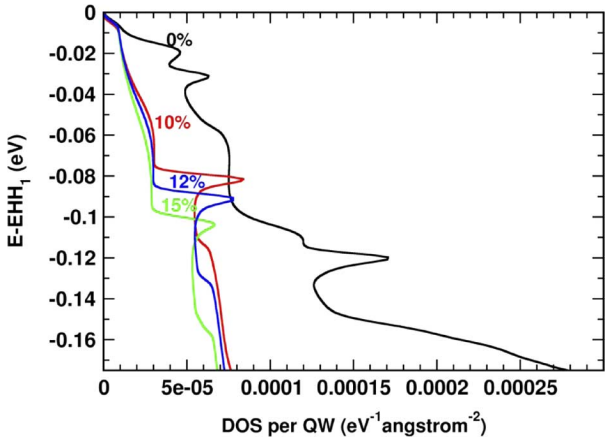

Fig. 2. Valence band density of states for the QW structures defined in Table I.

occurred by 10% In. We may therefore expect a significant reduction in $n_{\rm tr}$ and increase in differential gain by 10% In, with the addition of further In up to 15% then bringing a further small improvement in laser characteristics.

Fig. 3 shows the calculated variation of peak modal gain $g_{{\rm mod},w}$ and differential peak modal gain $dg_{{\rm mod},w}/dn_{\rm 2D}$ per QW as a function of the in-plane carrier density per QW, $n_{\rm 2D}$ at 25 °C (300 K). The total modal gain $g_{\rm mod}$ necessary to overcome cavity losses and start lasing has been calculated as 15.7 cm^{-1} at RT for an active material with five QWs of composition $In_{0.10}Ga_{0.90}As$ and QW width $L_w = 4$ nm (using a cold cavity model for the mirror losses). A three-QW system would then require $g_{{\rm mod},w} = 5.2$ cm^{-1} per QW and a six-QW system would require $g_{{\rm mod},w} = 2.6$ cm^{-1} per QW to reach threshold. We see in Fig. 3 that because of the reduced density of valence states, the calculated transparency sheet carrier density per QW, $n_{\rm tr,2D}$, decreases from 1.7×10^{12} cm^{-2} in an 8-nm GaAs QW to 1.35×10^{12} cm^{-2} in a 4-nm $In_{0.10}Ga_{0.90}As$ QW. The horizontal lines in Fig. 3 show the calculated threshold modal gain (per QW) for a VCSEL containing three, five, and six QWs, respectively. The threshold sheet carrier density decreases and 2-D differential modal gain also increases with increasing In content.

The modal gain per QW, $g_{{\rm mod},w}$, is related to the material gain $g_{\rm mat}$ as $g_{{\rm mod},w} = g_{\rm mat}\Gamma/N_w$, where Γ is the optical confinement factor and N_w is the total number of QWs. We use the differential material gain calculated with respect to the 3-D carrier density in the QWs, $dg_{\rm mat}/dn$ when comparing with experiments below. This is related to the differential modal gain

TABLE III
CALCULATED THRESHOLD SHEET CARRIER DENSITY PER QUANTUM WELL ($n_{\rm th}$) AND DIFFERENTIAL MATERIAL GAIN ($dg_{\rm mat}/dn$) AT THE THRESHOLD CARRIER DENSITY FOR THE ACTIVE REGION DESIGNS IN TABLE I. NUMBERS IN PARENTHESES ARE AT 85 °C, OTHERS AT 25 °C

QW material	QW width (nm)	No. of QWs	Barrier material	n_{th} (10^{12} cm^{-2})	dg_{mat}/dn (10^{-16} cm^2)
GaAs	8.0	3	Al(0.30)GaAs	2.17 (2.70)	7.9 (6.1)
In(0.10)GaAs	4.0	5	Al(0.37)GaAs	1.53 (1.87)	15.0 (11.9)
In(0.12)GaAs	3.6	5	Al(0.37)GaAs	1.49 (1.82)	15.8 (12.6)
In(0.15)GaAs	3.3	6	Al(0.37)GaAs	1.40 (1.71)	16.2 (13.1)

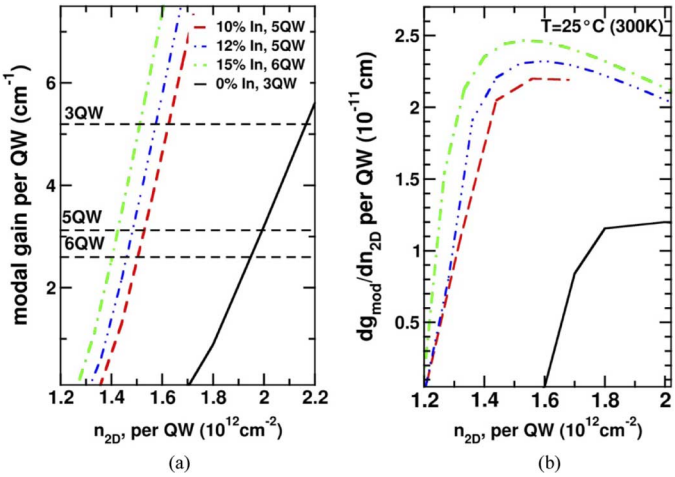

Fig. 3. Variation of (a) peak modal gain and (b) differential modal gain with sheet carrier density at 25 °C for the QW structures defined in Table I.

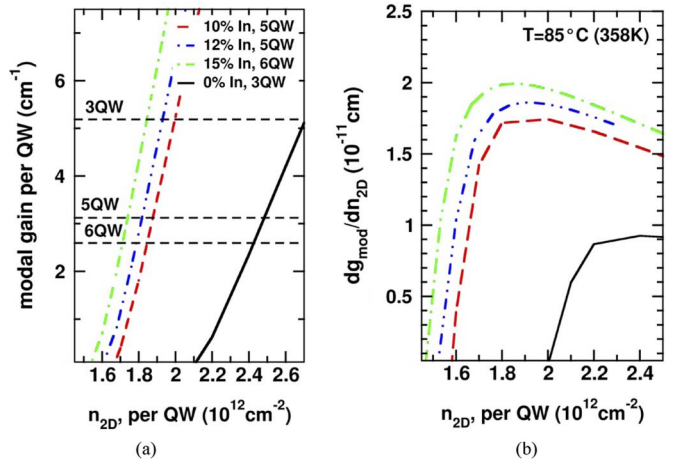

Fig. 4. Variation of (a) peak modal gain and (b) differential modal gain with sheet carrier density at 85 °C for the QW structures defined in Table I.

presented in Fig. 3 as $dg_{\rm mat}/dn = N_w L_w/\Gamma \times dg_{{\rm mod},w}/dn_{\rm 2D}$. Because $N_w L_w/\Gamma$ is approximately constant, we then find the same variation in the differential modal gain and differential material gain. We see from Fig. 3 that the calculated differential gain per QW at threshold increases from $dg_{{\rm mod},w}/dn_{\rm 2D} = 1.15$ to 2.18×10^{-11} cm ($dg_{\rm mat}/dn = 7.9$ to 15.0×10^{-16} cm^2) as the In content increases from 0% in a three-QW structure to 10% in a five-QW structure. The calculated differential gain at threshold is further increased to $dg_{{\rm mod},w}/dn_{\rm 2D} = 2.35 \times 10^{-11}$ cm ($dg_{\rm mat}/dn = 16.2 \times 10^{-16}$ cm^2) when the In content is increased to 15% in a six-QW structure. It can be observed from Fig. 3 that an increase from five to six QWs has little effect on the calculated threshold carrier density or differential gain per QW.

Fig. 4 shows the calculated variation of peak modal gain and differential peak modal gain per QW at 85 °C (358 K) as a function of carrier density. It can be seen that both the peak gain and differential gain show broadly similar trends to that observed in Fig. 3. We calculate that a significant improvement in differential gain is obtained by adding 10% In (90% improvement at 25 °C and 95% at 85 °C for a five-QW VCSEL), with a further increase of 6% (10%) at 85 °C relative to the 10% In value when the In content is increased to 12% (15% and six QWs). We conclude, therefore, that the improvement in differential gain is most marked with the initial addition of 10% In but that, so long as material quality is maintained, a small further improvement in the gain characteristics can be achieved through the use of higher In composition QWs. Table III summarizes the calculated variation in threshold carrier density and differential material gain as a function of In composition and QW width.

IV. EXPERIMENTS

The calculations in Section III predict a near doubling of the differential gain at threshold with five 4.0-nm $In_{0.10}Ga_{0.90}As/Al_{0.37}Ga_{0.63}As$ QWs compared to three 8-nm $GaAs/Al_{0.30}Ga_{0.70}As$ QWs. To confirm this improvement, high speed VCSELs were fabricated and values for the differential gain were deduced from small signal modulation response measurements.

The epitaxial VCSEL material was grown by MOCVD (AIX2600G3) by IQE Europe, paying special attention to accurate calibrations of QW thickness and strain to avoid relaxation and generation of dislocations. The VCSELs (multimode) employ a double oxide aperture, with a diameter of 9 μm, for current and optical confinement [1]. A double oxide aperture is used to reduce the capacitance associated with the oxide layers. The device capacitance is further reduced by a thick layer of BCB under the p-bond pad. Apart from the active region, the designs of the two VCSELs are identical. Output power and voltage, measured as a function of current, are shown in Fig. 5. The VCSELs exhibit quite similar dc characteristics with a threshold current of ~0.5 mA, a slope efficiency of 0.7–0.8 W/A, a maximum power of ~9 mW, and

TABLE IV
COMPARISON OF DIFFERENTIAL MATERIAL GAIN (dg_{mat}/dn) OBTAINED FROM THEORY AND MEASUREMENTS FOR TWO OF THE ACTIVE REGION DESIGNS IN TABLE I. NUMBERS IN PARENTHESIS ARE AT 85 °C, OTHERS AT 25 °C

Active region design	dg_{mat}/dn from theory (10^{-16} cm^2)	dg_{mat}/dn from measurements (10^{-16} cm^2)
3 x 8 nm GaAs QWs, 8 nm Al(0.3)GaAs barriers	7.9 (6.1)	7.5 (5.8)
5 x 4 nm In(0.10)GaAs QWs, 6 nm Al(0.37)GaAs barriers	15.0 (11.9)	18.0 (13.0)

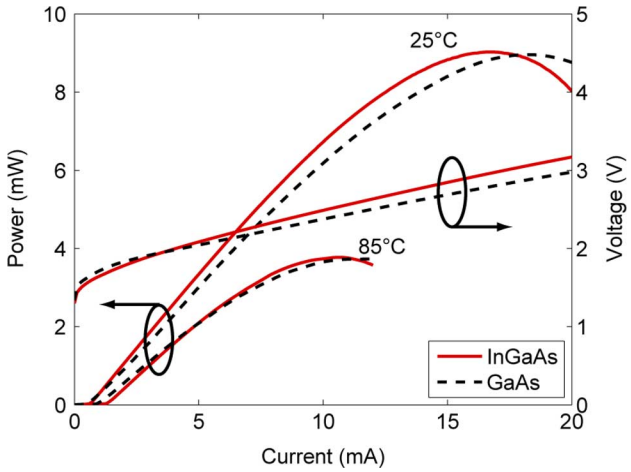

Fig. 5. Output power as a function of current at 25 and 85 °C for a VCSEL with a 3 × 8-nm GaAs/$Al_{0.30}Ga_{0.70}As$ active region (dashed) and a 5 × 4-nm $In_{0.10}Ga_{0.90}As/Al_{0.37}Ga_{0.63}As$ active region (solid). The voltage drop at 25 °C is also shown.

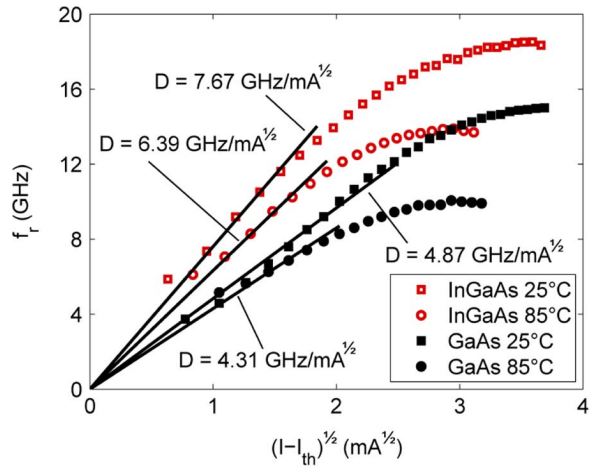

Fig. 6. Resonance frequency as a function of square root of current above threshold at 25 and 85 °C for the two VCSELs in Fig. 5.

a differential resistance of 70–80 Ω. The emission wavelength is at 845–850 nm.

The small-signal modulation response was measured at different bias currents and temperatures (25 °C and 85 °C) using the procedures outlined in [1]. From fits of a three-pole transfer function to the measured modulation response at each current, the resonance frequency (f_r) and its dependence on current (I) was deduced. The results are shown in Fig. 6.

The rate at which the resonance frequency increases with current above threshold (I_{th}) is quantified by the D-factor [1]

$$f_r = D \cdot \sqrt{I - I_{\mathrm{th}}} \tag{1}$$

where

$$D = \frac{1}{2\pi} \cdot \sqrt{\frac{\eta_i \Gamma v_g}{q V_a} \cdot \frac{dg_{\mathrm{mat}}/dn}{\chi}}. \tag{2}$$

The D-factors are obtained from the linear dependence of the resonance frequency on the square root of current above threshold at low currents and are shown in Fig. 6. The deviation from linearity at higher currents is due to thermal effects. It is obvious from the much higher D-factors for the VCSEL with strained InGaAs/AlGaAs QWs that such QWs provide higher differential gain (dg_{mat}/dn). To obtain numerical values for the differential gain from (2), all values for the device specific parameters in (2) have to be quantified. The optical confinement factors (Γ) were obtained from transfer matrix calculations and are listed in Table I. The active region volumes (V_a) were calculated from the number of QWs, their thicknesses and the diameter of the double oxide aperture. The transport factor (χ) was set to unity because of the relatively thin, graded composition separate confinement layers employed [17]. A value of 1×10^8 m/s was used for the group velocity (v_g) [18]. Accurate values for the internal quantum efficiency (η_i) and its dependence on temperature are more difficult to obtain. Assuming a temperature independent internal quantum efficiency of 90% for both VCSELs (which is a typical number for edge emitting lasers with a similar active region design [19]), we obtain the values for differential material gain listed in Table IV. The values are in very good agreement with those obtained from the calculations (also listed in Table IV) and confirm the predicted doubling of the differential material gain with strained InGaAs/AlGaAs QWs from 7.5×10^{-16} to 18×10^{-16} cm^2 at 25 °C and from 5.8×10^{-16} to 13×10^{-16} cm^2 at 85 °C. If we instead use the calculated values for differential material gain to obtain the internal quantum efficiency from the measured D-factors we obtain an internal quantum efficiency of 100% (77%) at 25 °C (85 °C) for the VCSEL with strained InGaAs/AlGaAs QWs and 94% (69%) at 25 °C (85 °C) for the VCSEL with unstrained GaAs/AlGaAs QWs. These are also reasonable values with the higher values for the VCSEL with InGaAs/AlGaAs QWs consistent with the larger barrier height.

V. Conclusion

In summary, we have shown that incorporating 10% In in the active region of an InGaAs/AlGaAs 850-nm VCSEL structure can lead to a significant improvement in the differential gain of the device compared to a GaAs/AlGaAs structure, both because of the strain-induced splitting of the HH and LH band edge states, and also because of the reduction in QW width required to maintain a fixed emission wavelength. Excellent agreement was obtained between the calculated and measured values of the differential gain, including its variation with In composition. We calculate that the incorporation of more In only brings a marginal further improvement to the differential gain. The 4-nm-wide strained $In_{0.10}Ga_{0.9}As$ QWs reported here are, therefore, close to optimum and are well below the critical thickness for layers with this level of strain, confirming the benefits of a strained InGaAs QW active region for reliable high-speed VCSEL devices and applications.

References

[1] P. Westbergh, J. S. Gustavsson, Å. Haglund, M. Sköld, A. Joel, and A. Larsson, "High speed, low current density 850 nm VCSELs," *IEEE J. Sel. Topics Quantum Electron.*, vol. 15, no. 3, pp. 694–703, 2009.

[2] Y.-C. Chang and L. A. Coldren, "Efficient, high data rate, tapered oxide aperture vertical cavity surface emitting lasers," *IEEE J. Sel. Topics Quantum Electron.*, vol. 15, no. 3, pp. 704–715, 2009.

[3] S. A. Blokhin, J. A. Lott, A. Mutig, G. Fiol, N. N. Ledentsov, M. V. Maximov, A. M. Nadtochiy, V. A. Shchukin, and D. Bimberg, "850 nm VCSELs operating at bit rates up to 40 Gbit/s," *Electron. Lett.*, vol. 45, no. 10, pp. 501–503, 2009.

[4] T. Anan, N. Suzuki, K. Yashiki, K. Fukatsu, H. Hatakeyama, T. Akagawa, K. Tokutome, and M. Tsuji, "High speed 1.1 μm range InGaAs VCSELs," in *Proc. Optical Fiber Communication Conf.*, San Diego, CA, 2008, paper OThS5.

[5] E. P. O'Reilly and A. R. Adams, "Band-structure engineering in strained semiconductor lasers," *IEEE J. Quantum Electron.*, vol. 30, no. 2, pp. 366–379, 1994.

[6] S. Weisser, E. C. Larkins, K. Czotscher, W. Benz, J. Daleiden, I. Esquivias, J. Fleissner, J. D. Ralston, B. Romero, R. E. Sah, A. Schönfelder, and J. Rosenzweig, "Damping limited modulation bandwidths up to 40 GHz in undoped short cavity In(0.35)Ga(0.65)As-GaAs multiple quantum well lasers," *IEEE Photon. Technol. Lett.*, vol. 8, no. 5, pp. 608–610, 1996.

[7] T. Aggerstam, R. Marcks Von Würtemberg, C. Runnström, and E. Choumas, "Large aperture 850 nm oxide confined VCSELs for 10 Gb/s data communication," in *Proc. SPIE*, 2002, vol. 4649, pp. 19–24.

[8] Y.-C. Chang, C. S. Wang, and L. A. Coldren, "High-efficiency, high-speed VCSELs with 35 Gbit/s error-free operation," *Electron. Lett.*, vol. 43, no. 19, pp. 1022–1023, 2007.

[9] R. H. Johnson and D. M. Kuchta, "30 Gb/s directly modulated 850 nm datacom VCSELs," in *Proc. Conf. Lasers Electro-Optics*, San Jose, CA, 2008, postdeadline paper CPDB2.

[10] P. Westbergh, J. S. Gustavsson, Å. Haglund, A. Larsson, F. Hopfer, G. Fiol, D. Bimberg, and A. Joel, "32 Gbit/s multimode fiber transmission using high speed, low current density 850 nm VCSEL," *Electron. Lett.*, vol. 45, no. 7, pp. 366–368, 2009.

[11] S. Tomic, E. P. O'Reilly, R. Fehse, S. J. Sweeney, A. R. Adams, A. D. Andreev, S. A. Choulis, T. J. C. Hosea, and H. Riechert, "Theoretical and experimental analysis of 1.3 μm InGaAsN/GaAs lasers," *IEEE J. Sel. Topics Quantum Electron.*, vol. 9, no. 5, pp. 1228–1238, 2003.

[12] M. Altarelli, U. Ekenberg, and A. Fasolino, "Calculations of hole subbands in semiconductor quantum wells and superlattices," *Phys. Rev. B.*, vol. 32, no. 8, pp. 5138–5143, 1985.

[13] I. Vurgaftman, J. R. Meyer, and L. R. Ram-Mohan, "Band parameters for III–V compound semiconductors and their alloys," *J. Appl. Phys.*, vol. 89, no. 11, pp. 5815–5875, 2001.

[14] M. P. C. M. Krijn, "Heterojunction band offsets and effective masses in III–V quaternary alloys," *Semicond. Sci. Technol.*, vol. 5, no. 1, pp. 27–31, 1991.

[15] S. B. Healy and E. P. O'Reilly, "Influence of electrostatic confinement on optical gain in GaInNAs quantum-well lasers," *IEEE J. Quantum Electron.*, vol. 42, no. 6, pp. 608–615, 2006.

[16] F. Szmulowicz, "Derivation of a general expression for the momentum matrix-elements within the envelope-function approximation," *Phys. Rev. B*, vol. 51, no. 3, pp. 1613–1623, 1995.

[17] R. Nagarajan, M. Ishikawa, T. Fukushima, R. S. Geels, and J. E. Bowers, "High speed quantum-well lasers and carrier transport effects," *IEEE J. Quantum Electron.*, vol. 28, no. 10, pp. 1990–2008, 1992.

[18] J. Y. Law and G. P. Agrawal, "Mode-partition noise in vertical-cavity surface-emitting lasers," *IEEE Photon. Technol. Lett.*, vol. 9, no. 4, pp. 437–439, 1997.

[19] S. Y. Hu, D. B. Young, S. W. Corzine, A. C. Gossard, and L. A. Coldren, "High efficiency and low threshold InGaAs/AlGaAS quantum well lasers," *J. Appl. Phys.*, vol. 76, no. 6, pp. 3932–3934, 1994.

Sorcha B. Healy is originally from Dublin, Ireland. She received an undergraduate degree in applied sciences (mathematics and physics) from the University of Dublin in 1997, studying at the Dublin Institute of Technology. Subsequently, she studied for the Master's degree in mathematical physics at the University College Dublin (1999), before moving to the University College Cork to work towards the Ph.D. degree with Prof. S. Fahy and Dr. C. Filippi (2003).

She currently works as a Staff Researcher with the Photonics Theory Group at the Tyndall National Institute, Cork. Her current research interests include gain and loss mechanisms of quantum dot and well heterostructures, and dilute nitride III–V materials.

Eoin P. O'Reilly was born in Dublin, Ireland. He received the B.A.(MOD.) degree in theoretical physics from Trinity College, Dublin, Ireland, and the Ph.D. degree in theoretical condensed matter physics at the University of Cambridge, Cambridge, U.K.

In 1984, he was appointed as a Lecturer at the University of Surrey, U.K., where he was head of the Department of Physics from 1997 to 2001. Since 2001, he has been with the Photonics Theory Group, Tyndall National Institute, University College Cork, Cork, Ireland, where he investigates the physics of next-generation photonic devices.

Prof. O'Reilly has been the Chairman of the Board of the European Physical Society (EPS) Condensed Matter Division since 2005.

Johan S. Gustavsson received the M.Sc. degree in electrical engineering and the Ph.D. degree in photonics from Chalmers University of Technology, Göteborg, Sweden, in 1998 and 2003, respectively. His Ph.D. dissertation dealt with mode dynamics and noise in vertical-cavity surface-emitting lasers (VCSELs).

Presently, he is an Assistant Professor at the Photonics Laboratory, Department of Microtechnology and Nanoscience, Chalmers University of Technology. His current research includes design, modeling, and characterization of long-wavelength semiconductor lasers, mode and polarization control in VCSELs using shallow surface structures, and improving the bandwidth of conventional GaAs-based VCSELs.

Petter Westbergh received the M.Sc. degree in engineering physics from Chalmers University of Technology, Göteborg, Sweden, in 2007. He is currently working towards the Ph.D. degree in optoelectronics at the Photonics Laboratory at Chalmers University of Technology.

His main research interests include fabrication and characterization of high-speed 850-nm vertical-cavity surface-emitting lasers (VCSELs) and wavelength-tunable VCSELs.

Åsa Haglund received the M.Sc. degree in physics from Gothenburg University, Gothenburg, Sweden, in 2000 and the Ph.D. degree in electrical engineering from Chalmers University of Technology, Göteborg, Sweden, in 2005. Her Ph.D. thesis was titled "Mode and Polarization Control in VCSELs Using Surface Structures."

Since 2008, she has been an Assistant Professor at the Photonics Laboratory, Department of Microtechnology and Nanoscience, Chalmers University of Technology. Her current research includes tunable VCSELs using MEMS structures, high-speed GaAs-based VCSELs, and deep-UV light emitters.

Anders Larsson received the M.Sc. and Ph.D. degrees in electrical engineering from Chalmers University of Technology, Göteborg, Sweden, in 1982 and 1987, respectively.

From 1984 to 1985, he was with the Department of Applied Physics, California Institute of Technology, Pasadena, and from 1988 to 1991, with the Jet Propulsion Laboratory, Pasadena, CA. In 1991, he joined the faculty at Chalmers University of Technology, where he was promoted to Professor in 1994. He has been a guest professor at Ulm University, Ulm, Germany, at the Optical Science Center, University of Arizona, Tucson, and at Osaka University, Osaka, Japan. He is presently a guest professor at the Institute of Semiconductors, Chinese Academy of Sciences. He has published 200 papers in scientific journals and 190 conference papers.

Dr. Larsson co-organized the IEEE Semiconductor Laser Workshop 2004, organized the European Semiconductor Laser Workshop 2004, and was the Program Chair for the IEEE International Semiconductor Laser Conference 2006 and the General Chair for the same conference in 2008. His scientific background is in the areas of materials and devices for optical communication, optical information processing, infrared detection, and optical measurements. Currently, his research is focused on vertical-cavity surface-emitting lasers, optically pumped semiconductor disk lasers, and emitters in wide bandgap materials. He is a fellow of the European Optical Society.

Andrew Joel is a graduate of the University College Cardiff.

He has over 20 years' experience working at the forefront of the design, development, and characterization of leading-edge compound semiconductor photonics and wireless products. He has a wealth of knowledge developing and volume manufacturing a wide range of lasers and detectors on multiple MOCVD platforms. He is currently Product Director of IQE Europe, Ltd. He was responsible for establishing IQE's successful development of leading-edge VCSELs. He has substantial experience of national and international collaborations with some of the world's leading academic and industrial organizations. He is joint author of several publications on photonics devices.